

Masticatory biomechanics and its relevance to early hominid phylogeny: An examination of palatal thickness using finite-element analysis

David S. Strait^{a,*}, Brian G. Richmond^b, Mark A. Spencer^c, Callum F. Ross^d,
Paul C. Dechow^e, Bernard A. Wood^b

^a Department of Anthropology, University at Albany, 1400 Washington Ave., Albany, NY 12222, USA

^b Center for the Advanced Study of Hominid Paleobiology, Department of Anthropology, The George Washington University,
2110 G St. NW, Washington, DC 20052, USA

^c School of Human Evolution and Social Change, Institute of Human Origins, Arizona State University, Box 874101, Tempe, AZ 85287-4101, USA

^d Department of Organismal Biology and Anatomy, University of Chicago, 1027 East 57th Street, Chicago, IL 60637, USA

^e Department of Biomedical Sciences, Baylor College of Dentistry, Texas A & M Health Science Center, 3302 Gaston Ave., Dallas, TX 75246, USA

Received 30 December 2005; accepted 21 November 2006

Abstract

It has been proposed that morphological characters functionally related to mastication may be unreliable indicators of early hominid phylogeny. One hypothesis states that masticatory characters are highly prone to homoplasy. A second hypothesis states that such characters are likely to be morphologically integrated and thus violate the assumption of character independence implicit in all phylogenetic analyses. Evaluation of these hypotheses requires that masticatory features be accurately identified, but, to date, there have been relatively few attempts to test precisely which early hominid features are functionally related to chewing. This paper uses finite-element analysis to evaluate the functional relationships of a character—palatal thickness—that is one of several *Paranthropus* synapomorphies putatively related to mastication. A finite-element model of 145,680 elements was created from sixty-one 2-mm-thick CT scans of a *Macaca fascicularis* skull. The model was assigned the elastic properties of facial bone and loaded with muscle forces corresponding to the moment of centric occlusion during mastication. The model was constrained so as to produce a reaction force (corresponding to the bite force) at M¹. With a few exceptions, the strain patterns in the finite-element model compare well with those gathered from published and unpublished bone-strain experiments. The model was then modified to have a thick palate. The model was reloaded using an identical loading regime, and the strain patterns of the original and thick-palate models were compared. Although a thickened palate acts to reduce palatal strain, strains are elevated in other facial regions. This suggests that a thick palate would not have evolved in isolation as an adaptation to withstand masticatory stress. Rather, a thick palate may have evolved in concert with a suite of other facial features that share a stress-resistance function. This appears to be consistent with hypotheses positing that at least some facial features related to chewing evolved in an integrated fashion. More functional studies of other facial features are needed, as are formal studies of morphological integration.

© 2007 Elsevier Ltd. All rights reserved.

Keywords: Homoplasy; Paranthropus; Finite-element analysis; Mastication; Biomechanics

Introduction

The concept of homoplasy is inseparable from the concept of phylogeny. To state that a character is homoplastic is also to state that two or more taxa are not as closely related as one

might expect given their similarity with respect to the character. Moreover, it is difficult, if not impossible, to determine a priori whether a character is homoplastic or homologous because, by definition, a homoplasy is a character that looks like a homology (Cracraft, 1981). Thus, in practice, homologies and homoplasies are identified as an a posteriori result of a phylogenetic analysis (e.g., Lauder, 1994; Kitching et al., 1998; Begun, 2007). Accordingly, this study examines

* Corresponding author. Tel.: +1 518 442 4717; fax: +1 518 442 5710.

E-mail address: dstrait@albany.edu (D.S. Strait).

homoplasy in early hominids within the context of the debate about the phylogenetic relationships of those species.

One of the principal debates in early hominid phylogeny concerns the question of whether the craniodental characteristics shared by the “robust” australopiths are synapomorphies or homoplasies. From the perspective of phylogenetic reconstruction, this question is equivalent to asking whether these hominids are monophyletic or polyphyletic. Resolution of this question depends largely on interpretations of traits thought to be functionally related to mastication. Phylogenies supporting *Paranthropus* polyphyly generally rely on the assumption that masticatory features are either highly prone to homoplasy or are morphologically integrated such that they represent only one or a few complexes whose weight in a cladistic analysis is minimal. However, although the “robust” australopiths unquestionably share a number of derived craniofacial features, the inferred functional relationships of those features have rarely been rigorously investigated. Many of these features are thought to be related to mastication (e.g., Robinson, 1954, 1963; Jolly, 1970; Grine, 1981; Rak, 1983; Skelton and McHenry, 1992), but the complex architecture of the face has largely precluded attempts to evaluate these functional inferences. If the functional inferences are false, then the phylogenetic hypotheses based upon them may be false as well. This paper uses an engineering method, finite-element analysis (FEA), to test the functional relationships of one of the characters—palatal thickness—relevant to this debate.

Mastication and early hominid phylogeny

Prior to the discovery of KNM-WT 17000 (the “Black Skull”), the question of “robust” australopith monophyly was hardly a critical phylogenetic issue. Indeed, although two “robust” species were recognized, it was not uncommon to see them depicted in phylogenetic trees as a single taxon, “*P. boisei* + *P. robustus*” (e.g., White et al., 1981). Following the discovery of KNM-WT 17000, a consensus concerning “robust” australopith relationships has been lacking.

In their description of KNM-WT 17000, Walker et al. (1986) noted that the specimen shared a few derived features exclusively with fossils of *P. boisei* that were known from chronologically younger strata. This suggested to them that the specimen was plausibly an early member of the *P. boisei* lineage. However, this would imply that *P. robustus* was excluded from this lineage because such features were lacking in the southern African species. Thus, *P. robustus* was considered a probable descendant of *A. africanus*, indicating that the many derived features shared between *P. robustus* and *P. boisei* must have evolved in parallel. Walker et al. (1986) suggested that such a scenario is possible because the features presumed to be homoplastic are all related to mastication, and thus they should be prone to evolve in parallel (but see Collard and Wood, 2001, 2007).

The discovery of KNM-WT 17000 also coincided with the widespread application of numerical cladistic methods in paleoanthropology (e.g., Chamberlain and Wood, 1987).

Subsequent cladistic analyses of early hominids have all found that *P. boisei* and *P. robustus* are more closely related to each other than to non-“robust” hominids, but their relationships to *P. aethiopicus* (represented by KNM-WT 17000) remain controversial. Wood (1988) showed that a cladistic analysis using the data set published by Walker et al. (1986) resulted in *Paranthropus* polyphyly, with *P. boisei* and *P. robustus* being sister taxa but *P. aethiopicus* being more distantly related (i.e., the sister taxon of a clade comprising all hominids except *Praeanthropus afarensis*). In a subsequent and morphologically more exhaustive study, Skelton and McHenry (1992) obtained an identical tree. They (Skelton and McHenry, 1992) noted that masticatory and nonmasticatory traits appeared to support different phylogenies. Moreover, they reasoned that masticatory features were both overrepresented in hominid trait lists and unlikely to be independent because they were all related to a common function (see also Skelton et al., 1986). Character independence is a crucial assumption of cladistic analysis, and thus, in their view (Skelton and McHenry, 1992), characters related to “heavy chewing” were likely to bias results in favor of *Paranthropus* monophyly. Because of these apparent deficiencies, Skelton and McHenry (1992) concluded that masticatory features may be unreliable indicators of phylogeny in early hominids.

Although other phylogenetic analyses have supported *Paranthropus* monophyly (Wood, 1991, 1992; Strait et al., 1997; Strait and Grine, 1999, 2001, 2004), these all explicitly or implicitly assumed that masticatory features are independent of each other, and that they are no more prone to homoplasy than are other craniodental characters. Thus, interpretations about “robust” australopith relationships depend critically on how one interprets features that are functionally related to chewing. However, this raises another issue: When one speaks of masticatory features, precisely which features are being discussed? For example, Strait and Grine (1998) identified 30 masticatory features in their (Strait et al., 1997) data set, while Skelton and McHenry (1998) identified 26; only 17 of these were considered chewing features by both sets of authors, and 13 of Strait and Grine’s (1998) chewing features and 9 of Skelton and McHenry’s (1998) were not recognized as such by the other researchers. Thus, there was disagreement concerning the functional relationships of 22 characters, representing more than a third of Strait and Grine’s (1998) entire 60-character data set.

There is widespread agreement that evolutionary trends in the masticatory apparatus play an important role in early hominid evolution (e.g., Robinson, 1963; Jolly, 1970; Grine, 1981; Walker, 1981; Rak, 1983), so why is it that two sets of researchers (Skelton and McHenry, 1998; Strait and Grine, 1998) can disagree so fundamentally about which traits are functionally related to chewing? One possible answer is that hypotheses about facial function are difficult to test. Unlike the mandible, which has a relatively simple geometry, the facial skeleton has a complex architecture that defies simple attempts to model it biomechanically. Thus, although hypotheses about facial function abound (e.g., Endo, 1966;

Greaves, 1985; Preuschoft et al., 1986; Thomason and Russell, 1986), and although some of these that are specifically related to hominids have been highly influential (e.g., Rak, 1983), these hypotheses are either untested or have not been supported by experimental data (e.g., Hylander et al., 1991; Ross and Hylander, 1996). Thus, it is fair to say that the masticatory significance of many osseous features of the early hominid face is unclear, and this has made it difficult to evaluate the phylogenetic relationships of the “robust” australopiths.

The character evolution of palatal thickness

Palatal thickness is an example of a phylogenetically significant character that is putatively related to mastication. “Robust” australopiths are unique among hominids in having exceptionally thick palates (e.g., McCollum et al., 1993). Rak (1983) hypothesized that a thick palate acts to resist shear imposed by unilateral chewing. Consequently, palatal thickness is among the masticatory features that Walker et al. (1986) consider prone to evolve in parallel and that Skelton and McHenry (1992) consider likely to be functionally integrated with each other. Thus, in a phyletic tree consistent with Walker et al.’s (1986) hypothesis (Fig. 1A), thick palates evolve homoplastically in the *P. robustus* and *P. aethiopicus* + *P. boisei* lineages. In the cladogram proposed by Skelton and McHenry (1992), they evolve in parallel in the *P. aethiopicus* and *P. boisei* + *P. robustus* clades (Fig. 1B). Alternatively, in analyses in which putative masticatory characters are considered independent traits, a thick palate is one of many synapomorphies supporting a “robust” clade. For example, in the phylogenetic hypothesis of Strait and Grine (2004), a hyperthick palate evolves in the last common ancestor of *Paranthropus* (Fig. 1C) (see also Strait et al., 1997; Strait and Grine, 1999, 2001).

In contrast, McCollum (1999) suggested that palatal thickness is neither an independent character, nor is it functionally related to mastication. Rather, thickness is a nonfunctional consequence of developmental constraints related to vomeral position, and thus it is developmentally (rather than functionally) integrated with a suite of nonmasticatory characters. McCollum (1999) did not propose a formal phylogenetic hypothesis, but the implication of her developmental hypothesis is that the number of independent characters supporting *Paranthropus* monophyly is overstated, and therefore polyphyly is a reasonable hypothesis. If so, then features like palatal thickness may have evolved in parallel in polyphyletic “robust” clades.

Insofar as palatal thickness is representative of a large class of characters that might be both synapomorphies of *Paranthropus* and functionally related to mastication, it is clear that testing the functional relationships of these characters will have a major impact on phylogenetic hypotheses. If the characters are not functionally related to mastication, then phylogenies in which they are assumed to be either functionally integrated or prone to homoplasy can be correspondingly discounted.

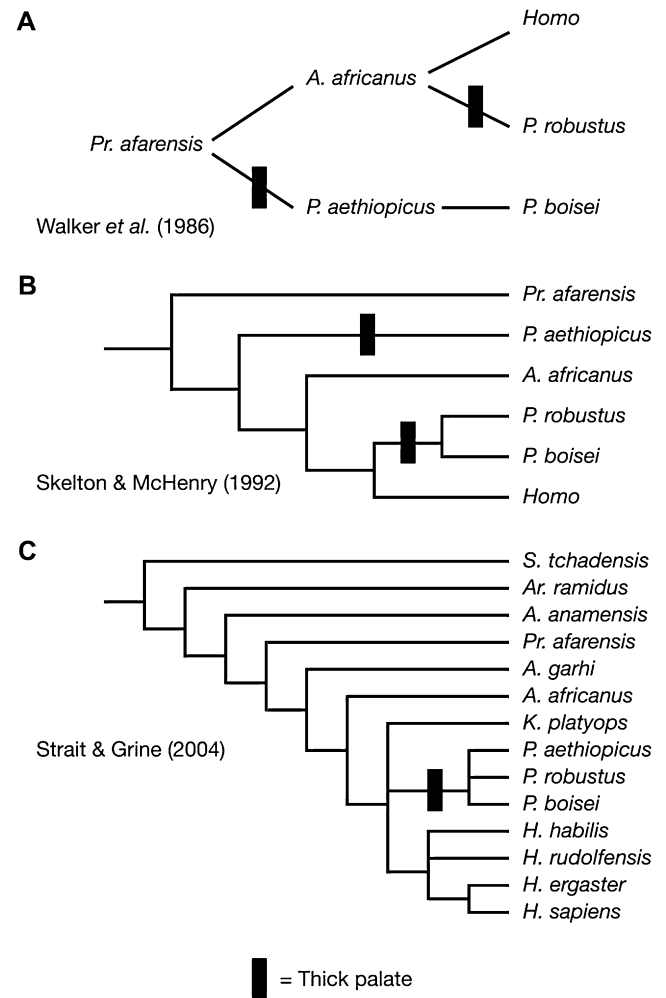


Fig. 1. Character evolution of palatal thickness in early hominids. Black rectangles represent the evolution of a thick palate. (A) Phyletic tree implied by Walker et al. (1986). (B) Cladogram of Skelton and McHenry (1992). (C) Cladogram of Strait and Grine (2004). A thick palate evolves homoplastically in A and B.

Functional hypothesis

The hypothesis tested here is that increased palatal thickness is an adaptation to resist elevated shear stress during mastication (Rak, 1983). This will be tested using finite-element analysis (FEA) by comparing results from similar models in which the relevant feature, the palate, has been modified. Finite-element analysis is a widely used engineering and biomechanical technique (e.g., Huiskes and Chao, 1983; Cook et al., 1989; Gross et al., 1992) that has recently come to the attention of paleoanthropologists and paleontologists (e.g., Koriath et al., 1992; Borrazzo et al., 1994; Spears and Crompton, 1994, 1996; Richmond and Qin, 1996; Ross and Chen, 1997; Ryan and Kappelman, 1997; Chen and Chen, 1998; Richmond, 1998; Rayfield et al., 2001; Richmond et al., 2005). Finite-element analysis should not be confused with finite-element scaling analysis (FESA), which is a method concerned with quantifying shape differences (Cheverud et al., 1983; Richtsmeier et al., 1992). Rather, FEA is a tool

for studying the response of an object or tissue to an applied load (Fig. 2).¹

Two finite-element (FE) models of a *Macaca fascicularis* skull were created—one with a regular (thin) palate and one with an abnormally thick palate. The models were assigned the elastic properties of facial bone and subjected to simulated bites using muscle forces derived from experimental studies (Ross et al., unpublished data). Resulting patterns of stress and strain were observed. The functional hypothesis predicts that maximum shear strains in the palate will be substantially lower in the model with the thick palate. If not (i.e., if palatal strains are broadly similar in the two models), then the functional hypothesis is rejected, and one may conclude that palatal thickness is unrelated to force resistance during mastication.

Materials and methods

Sample

The finite-element models were based on the skull of a male *M. fascicularis* specimen housed at the U.S. National Museum of Natural History. *Macaca fascicularis* was chosen because this species has been the subject of prior studies of masticatory bone strain (e.g., Hylander, 1984; Hylander et al., 1991; Borrazzo et al., 1994; Hylander and Johnson, 1997; Ross, unpublished data). Sixty-one 2-mm-thick CT scans were obtained from the specimen. Scans were digitized using reverse-engineering software, and a virtual solid model was created (Fig. 3A).

Mesh creation

During mesh creation, a complex object is modeled as a virtual mesh of many small, simple elements. These elements generally take the form of bricks or tetrahedra. The elements are linked at their corner points, called nodes, and strains are generated as the nodes are displaced. In the present study, the NORMAL (thin palate) model of the macaque skull was constructed using 145,480 polyhedral brick elements containing between four and eight nodes each (Fig. 3B). Note that an updated version of this model has been published elsewhere (Strait et al., 2005; Ross et al., 2005), but the differences between that model and the present one should not have a profound impact on the results. When the NORMAL model was modified to have a thick palate (THICK model), the newly generated mesh contained 290,639 elements. The discrepancy

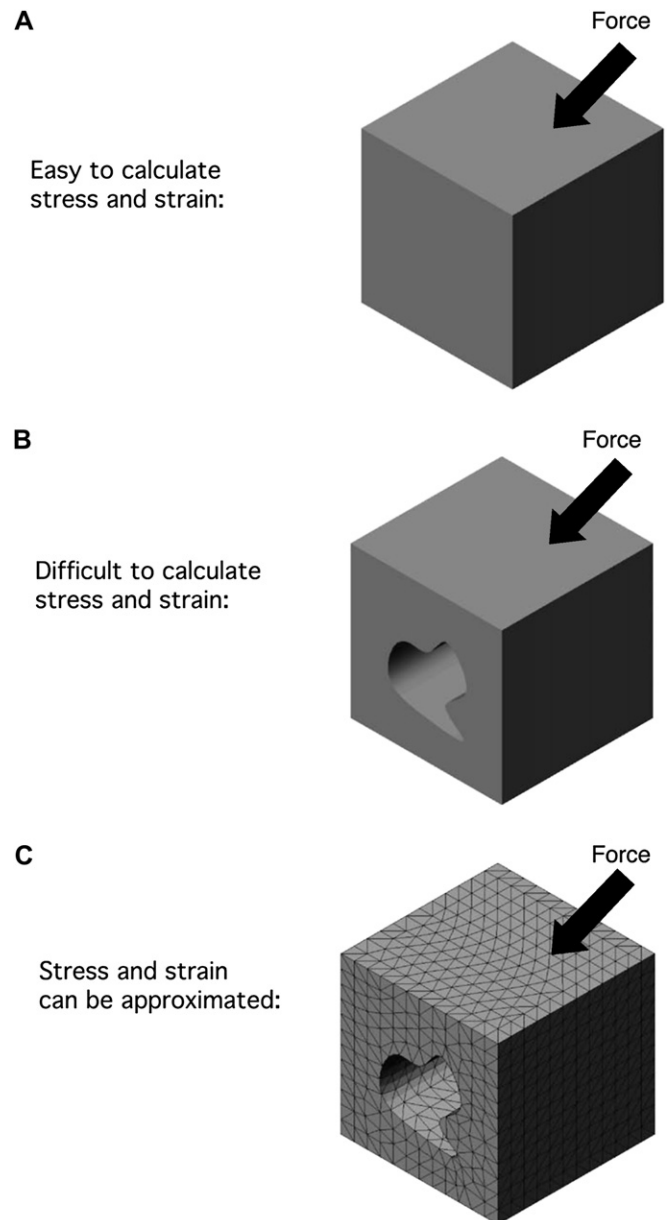


Fig. 2. Finite-element analysis is useful for computing stress and strain in objects with complex geometry. (A) Force is applied to an object of simple geometry, for which stress and strain are easily computed. (B) Force is applied to an object of complex geometry, but stress and strain are difficult or impossible to calculate exactly. (C) Force is applied to a model of the complex object. The model is composed of many elements, each of simple geometry. Stress and strain can be computed at each node defining the elements, and when elements are viewed collectively, stress and strain in the model approximates that of the object.

in element number is due to the fact that the geometry of the model is so complex that even minor modifications in shape can have a profound effect on the automated mesh-generating process and the resulting element configuration. In general, models with higher mesh density (i.e., with more elements and nodes) more closely approximate the structure's exact geometry. More important than the absolute number of elements is the concentration of elements in regions that are likely to experience high strain gradients due to their geometry

¹ In mechanical terms, the application of a load results in stresses and strains in the structure. **Stress** (σ) is defined as force per unit area (F/A) and is a measure used to describe the internal forces in an object (Currey, 1984; Cowin, 1989). **Strain** (ϵ) describes the deformations that result from an imposed load and is defined as the change in length divided by original length ($\Delta L/L$). By convention, stretching a bone in tension is a positive strain and compression is a negative strain. The greatest tensile strain at a given point is termed maximum principal strain, and the greatest compressive strain is termed minimum principal strain. Maximum shear strain is calculated as maximum principal strain minus minimum principal strain.

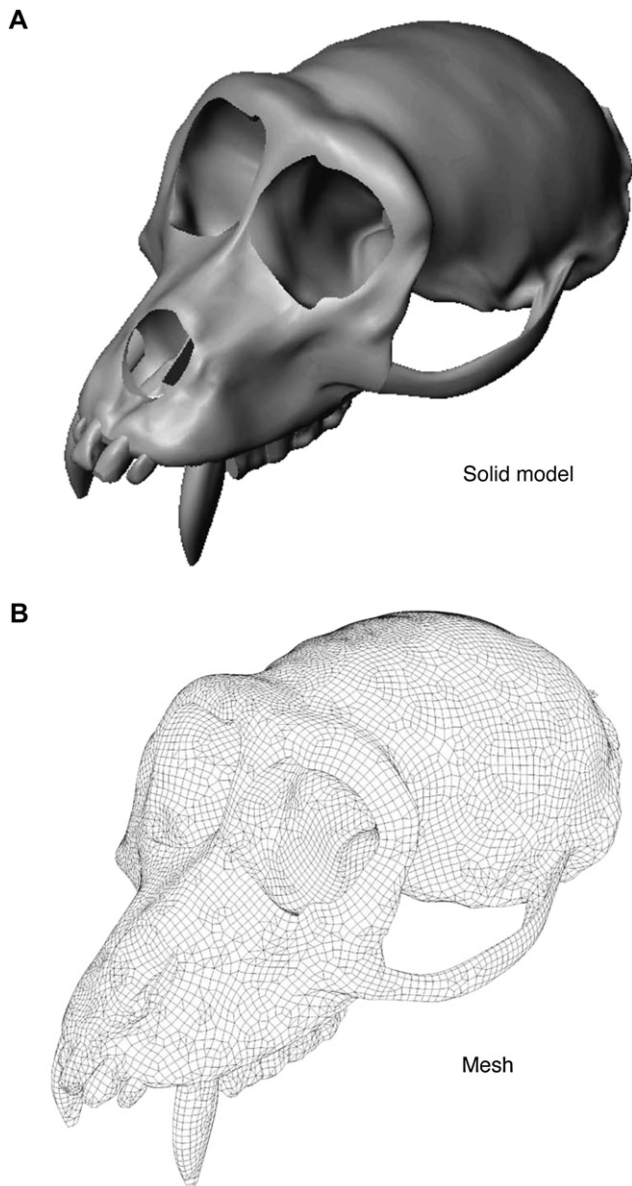


Fig. 3. Solid model (A) and finite-element mesh (B) of a *M. fascicularis* skull.

(Cook et al., 1989), such as irregularities or margins of holes. Both the NORMAL and THICK models satisfy this criterion with relatively high element densities in tightly curved regions such as the nasal aperture (see Fig. 6). The correspondence between the NORMAL model and the experimental strain values provides evidence to suggest that the mesh density of the NORMAL model is sufficiently refined (see validation section). When constructing the model, the skull was aligned such that the occlusal plane was horizontal (i.e., in the x - z plane).

Boundary conditions

Boundary conditions refer to the loads, constraints, and elastic properties applied to a model. Eight muscle forces were applied to the mesh, representing the right and left

anterior temporalis, superficial masseter, deep masseter, and medial pterygoid. These are the muscles that are principally responsible for jaw elevation during mastication. Muscle-force magnitudes and orientations are summarized in Table 1. Force orientation was estimated by measuring the relative positions of muscle origins and insertions, and by examining muscle maps based on dissections (Anton, 1993). Muscle-force magnitude was estimated by combining data on muscle activity and physiological cross-sectional area. Within vertebrates, myofibrillar cross-sectional area is the closest correlate of force-generating capacity (Murphy, 1998). Area and force are related such that approximately 300 kiloNewtons are produced for every square meter of striated muscle (Murphy, 1998). Area data were obtained from Anton (1993). However, Anton (1993) did not collect data for the anterior temporalis in *M. fascicularis*. Thus, Anton's (1993) data for *M. mulatta* were used instead. *Macaca mulatta* is larger than *M. fascicularis*, and, as a result, the muscle-force magnitudes employed in the model slightly overestimate the forces actually generated by *M. fascicularis*.

Measurements of cross-sectional area do not by themselves provide reliable estimates of muscle force because at any given moment, different muscles may have very different levels of activity. The relative force magnitudes exerted by each muscle at or near centric occlusion were calculated by assuming that force production is proportional to the magnitude of muscle activity, as measured by the root mean square (r.m.s.) of electromyography (EMG) data collected during chewing experiments (Ross, 2001). The highest standardized r.m.s. EMG activity recorded from each electrode during an experiment is assigned a value equal to 100% of the cross-sectional area; when the muscle is acting at less than peak activity (e.g., at 50% of peak), then force is proportional to a corresponding percentage of cross-sectional area. Electromyography data gathered simultaneously from all eight muscles enable relative force magnitudes to be generated.

In FEA, loads are translated into strains instantaneously. When investigating chewing, a logical instant to model is the moment at which bite force is maximized. Bone-strain

Table 1
Muscle forces applied to finite-element model

Muscle	Magnitude in Newtons	Orientation vector (x, y, z) ¹
Superficial masseter		
Working-side	70.627	(-0.2, -1, -0.2)
Balancing-side	34.682	(0.2, -1, -0.2)
Deep masseter		
Working-side	22.591	(-0.6, -1, 0)
Balancing-side	8.214	(0.6, -1, 0)
Medial pterygoid		
Working-side	34.794	(0.75, -1, 0)
Balancing-side	6.904	(-0.75, -1, 0)
Anterior temporalis		
Working-side	36.592	(0.1, -1, -0.1)
Balancing-side	15.147	(-0.1, -1, -0.1)

¹ X-direction is positive to the left (working) side; y-direction is positive superiorly; z-direction is positive anteriorly.

magnitudes recorded from the lateral aspect of the mandibular corpus below M_{1-2} in macaques are highly correlated with the magnitude and timing of bite force during isometric biting on a force transducer ipsilateral to the strain gage (Hylander, 1986), so the timing of peak bite force was estimated using the timing of peak strain in the mandibular corpus. Root-mean-square EMG activity in the masseter (Hylander and Johnson, 1989) and temporalis muscles (Ross and Patel, unpublished data) precedes the force generated by those muscles by approximately 20 msec. Consequently, the muscle forces entered into the FEA were calculated from r.m.s. EMG activity 20 msec prior to the instant of peak corpus strain. In summary, muscle-force magnitude is calculated as: $F = (\text{cross-sectional area}) \times (300 \text{ kN/m}^2) \times (\% \text{ of peak activity 20 msec prior to peak corpus strain})$.

Three sets of constraints were applied to the model. Nodes at the right and left articular eminences and the crown of the left M^1 were fixed in place. When muscle forces are applied to a model with these constraints, the model is pulled inferiorly onto the fixed points. Reaction forces are generated at each location, simulating the contact between the mandibular condyles and articular eminences, and between the teeth and a food item. Obviously, in life, the masticatory muscles act principally to move the mandible rather than the cranium. However, in a free-body diagram, the masticatory muscle forces act to pull the skull down onto a bite point, producing strains in the face equivalent to those produced by pulling a mandible up onto a resistant food item, and then having the item contact a bite point on the maxillary tooth row. In either case, bite force is a reaction force at the bite point.

Elastic properties refer to the force-displacement relations of the substance being modeled, which in this case is facial bone. Bone presents a formidable modeling challenge not only because elastic properties vary at different locations across the skull (Peterson and Dechow, 2003), but also because bone is anisotropic, meaning that its elastic properties are not the same in all directions. The orientations and magnitudes of Young's modulus and Poisson's ratio were obtained from 25 locations on macaque skulls (Wang and Dechow, 2006).² As a simplification, bone was modeled isotropically, with the values of Young's modulus (19.8 GPa) and Poisson's ratio (0.315) representing averages of the respective values in the axis of maximum stiffness obtained at all locations on the face (16 of the 25 total locations). In other work, we have applied more precise elastic properties to an updated version of the current macaque model (Strait et al., 2005). That study demonstrated that the use of orthotropic elastic properties that varied by cranial region produced results that were more accurate than a model that used a single set of isotropic

properties (as is done here). However, although elastic properties affected strain magnitudes somewhat, broad-scale deformation patterns were not profoundly affected. Thus, although the results presented here could be refined by the use of more precise assumptions about elastic properties, the properties employed here should be adequate to derive the general deformation pattern of the skull.

Solution

The solution of an FEA entails calculating the displacements, strains, and stresses experienced by the model. These results are a product of the elastic properties of the model and the loads applied to it. Displacement data are presented by comparing the shape of the undeformed mesh to that of the mesh after it has been deformed by masticatory loads. Color mapping on the mesh indicates regions of high strain. In addition, the magnitude and orientation of strain are recorded at several nodes on the mesh (Fig. 4). Nodes 1–8 correspond to locations on the facial skeleton from which experimental strain data have been recorded. Nodes 9–18 correspond to locations in a coronal plane passing through the left M^1 (i.e., the bite point).

Validation

Validation entails testing the results of the model against empirical data obtained from experiments. Validation is a critical stage in FEA, because if model strains do not conform reasonably well to experimentally derived strains, then there is no reason to be confident in the accuracy of the model, and interpretation of the model is hindered (or made impossible). The strain data obtained from the NORMAL model were validated by comparing them to those obtained from published and unpublished chewing experiments (Hylander et al., 1991; Hylander and Johnson, 1997; Ross, 2001; Ross et al., 2002; Ross et al., unpublished data) (Table 2).

The model and experimental data differ in subtle ways that may affect validation. First, the published experimental data consist of peak strain values for a number of different regions on the facial skeleton. However, not all regions experience peak strain at the same time during the chewing cycle, and thus peak strains from different regions are not precisely simultaneous. In contrast, the strains derived from FEA represent strains at a particular instant in time (e.g., the instant of peak corpus strain). Thus, there is an expectation that the strains at that moment in time in other regions may be at least slightly below peak.

A second difference between the model and experimental data concerns dimensionality. Experimental strains are two-dimensional due to the fact that strains can only be measured within the plane of the gage. In contrast, model strains are three-dimensional, as are the strains actually experienced by the organism. Thus, experimental strains represent three-dimensional strains projected into two-dimensional space. If a given strain vector (e.g., maximum principal strain) has a strong directional component that is perpendicular or oblique

² The elastic, or Young's, modulus (E) is defined as stress divided by strain (σ/ϵ) in simple extension or compression. It, therefore, numerically describes the stiffness of a material. For example, rubber will strain (deform) far more than steel under a given amount of stress and it has a correspondingly lower E . Poisson's ratio is the lateral strain divided by axial strain, thus representing how much the sides of a material will contract as it is tensed (or, conversely, how the material will expand as it is compressed).

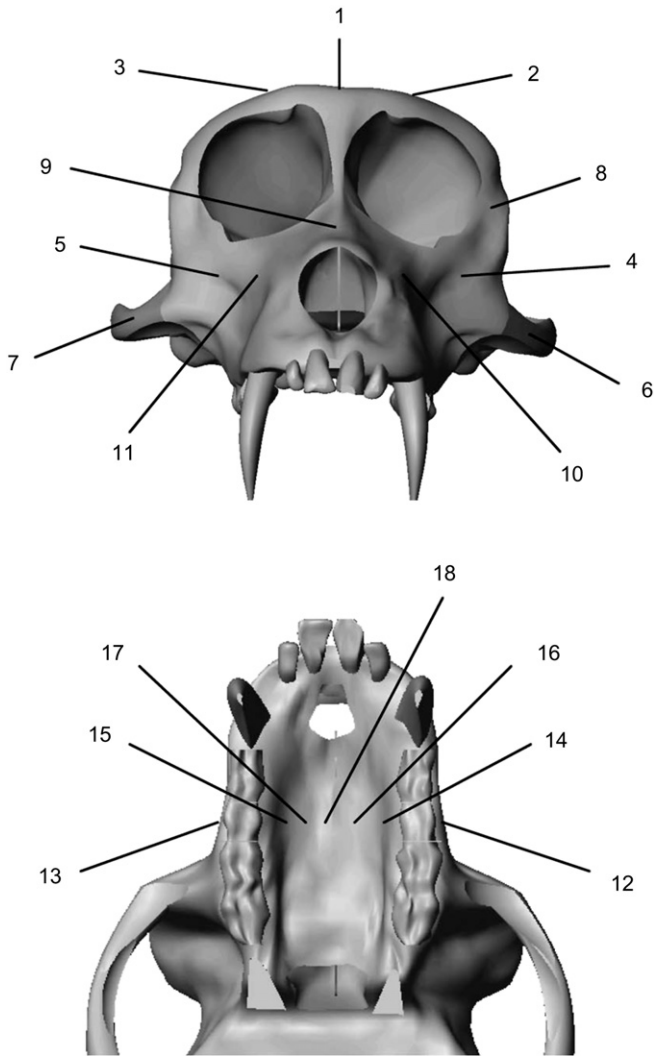


Fig. 4. Facial regions on the finite-element model from which strain data were tabulated. W = working-side; B = balancing-side; 1 = dorsal interorbital; 2 = W dorsal orbital; 3 = B dorsal orbital; 4 = W infraorbital; 5 = B infraorbital; 6 = W midzygomatic; 7 = B midzygomatic; 8 = W postorbital bar; 9 = dorsal rostral; 10 = W lateral rostral; 11 = B lateral rostral; 12 = W buccal alveolus; 13 = B buccal alveolus; 14 = W palatal margin; 15 = B palatal margin; 16 = W palatine process; 17 = B palatine process; 18 = midpalate. Experimental bone-strain data are available for regions 1–8.

to the gage, then the gage will underestimate the magnitude of the vector.

Experimentation

If a model can be validated, then it can be used in modeling experiments. Thus, after validating the NORMAL model by comparing its results with experimentally derived strain data, the results of the NORMAL model were compared with those of the THICK model. The palate in the THICK model is approximately twice as thick as that in the NORMAL model, which approximates the difference in thickness observed between “robust” and “gracile” australopiths (McCollum et al., 1993). The boundary conditions applied to the THICK model were equivalent to those of the NORMAL model. In

this way, it is possible to examine the biomechanical consequences of altering palatal geometry while controlling for other biomechanical variables. Maximum shear-strain magnitudes from equivalent locations on both models were compared.

Results

Solution

After loading, the general pattern of deformation experienced by the model is that the rostrum is twisted around an anteroposterior axis such that the balancing-side tooth row is displaced inferiorly (Fig. 5). The rostrum is also bent in a sagittal plane, but most of the stress is concentrated below the orbital region. The working-side orbit is slightly compressed top to bottom, while the balancing-side orbit is elongated in the same direction. Both zygomatic arches are deformed inferiorly by the forces of the masseter muscles. Deformation is greater in the working-side arch, presumably as a consequence of the greater masseter muscle force on that side, and because the bite point limits the inferior displacement of the working-side face. Corresponding to these gross patterns of deformation, tensile and compressive strain concentrations are observed across the face (Figs. 6–8). Strain magnitudes and orientations from selected facial regions are presented in Table 3. Overall, strain in the face is fairly low, with most regions experiencing maximum shear strains of less than 500 microstrain. Strains are higher in a few regions (zygomatic arch, maxilla just anterior and inferior to the zygomatic root), with shear-strain values approaching or exceeding 1,000 microstrain.

Validation

The pattern of deformation in the circumorbital region of the NORMAL model (see above) broadly matches that observed in experimental studies of anthropoid primates (Hylander et al., 1991; Ross and Hylander, 1996; Hylander and Johnson, 1997; Ross, 2001; Ross et al., 2002; Ross et al., unpublished data). Maximum shear strain magnitudes in the NORMAL model are comparable to those observed in experiments, and strains in most regions are reasonably close to average experimental values (Fig. 9). However, some regions have magnitudes that are lower (e.g., dorsal interorbital) or higher (e.g., middle of the working-side zygomatic arch) than might be expected given values in other regions. Orientations of the maximum principal strains in the NORMAL model tend to be within or just outside the observed variation in experimental values (Fig. 10). A notable exception concerns the orientation of the maximum principal strain in the working-side zygomatic arch, which has a more posterior orientation in *in vivo* experiments than is observed in the model. However, these experiments (Hylander and Johnson, 1997) also reveal that strain orientations in the arch exhibit a gradient such that orientations shift from anterosuperior to posterosuperior as one moves posteriorly along the arch. Thus, strain

Table 2
Validation data¹

Region	Reference	Experiment	Mean maximum shear strain (± 2 standard deviations, in microstrain)
1. Dorsal interorbital	Hylander et al. (1991)	5 AW	169 \pm 94
		5 AB	266 \pm 82
		6 W	185 \pm 78
		6 B	182 \pm 68
		2 AW	139 \pm 110
		2 AB	129 \pm 42
		2 BW	86 \pm 38
		5 BW	117 \pm 56
		5 CW	240 \pm 116
		5 CB	200 \pm 84
2. W Dorsal orbital	Hylander et al. (1991)	5 AW	100 \pm 61
		6W	85 \pm 44
3. B Dorsal orbital	Hylander et al. (1991)	5 AB	147 \pm 60
		6 B	105 \pm 29
4. W Infraorbital	Hylander et al. (1991), Ross et al. (2002), Ross et al. (unpublished data)	5 CW	613 \pm 256
		7	180 \pm 128
5. B Infraorbital	Hylander et al. (1991), Ross et al. (2002), Ross et al. (unpublished data)	5 CB	295 \pm 234
		7	192 \pm 160
6. W Midzygomatic	Hylander et al. (1991), Hylander and Johnson (1997)	2 AW	661 \pm 414
		2 BW	569 \pm 244
		5 BW	250 \pm 104
		2	857 \pm 360
		5	614 \pm 274
		7	398 \pm 204
		9	391 \pm 72
7. B Midzygomatic	Hylander et al. (1991), Hylander and Johnson (1997)	2 AB	352 \pm 238
		2	578 \pm 212
		5	440 \pm 254
		7	349 \pm 262
		9	202 \pm 168
8. W Postorbital bar	Ross et al. (unpublished data)	46	135 \pm 113
		47	194 \pm 197
		48	142 \pm 129

¹ In all experiments, “apple with skin” is the food item being chewed. W = working-side; B = balancing-side.

orientations in the middle of the arch in the NORMAL model resemble experimental strains from the posterior part of the arch. Overall, the NORMAL model appears to be deformed in a broadly realistic manner, and thus the model can be considered valid in most relevant features.

Experimentation

Compared to the NORMAL model, shear strains in the THICK model are lower within the palate (Fig. 11), but higher in most other facial regions (Table 4). The absolute differences in shear-strain magnitudes are generally low (less than 150 microstrain; see Fig. 12A), but the percentage differences are more substantial in many regions (Fig. 12B). Palatal strains decrease by 33–43% (regions 16–18), but strains in both palatal margins (regions 14 and 15) increase by 28%. Strains are elevated by 14–39% in circumorbital regions and the

working-side zygomatic arch (regions 1–6, 8). Strain in the balancing-side zygomatic arch is only modestly elevated (4%; region 7). The only nonpalatal regions that experience reduced shear strain in the THICK model are found on the sides of the rostrum, including the buccal surfaces of the alveoli (regions 11–13).

Discussion

Differences between models

It is not surprising that the THICK model experiences lower strains in the palate. Stress is calculated as force divided by the area over which it is applied (e.g., Wainwright et al., 1982), and thus, as the cross-sectional area of the palate increases, stresses and corresponding strains will decrease. However, the increases in strain observed in many

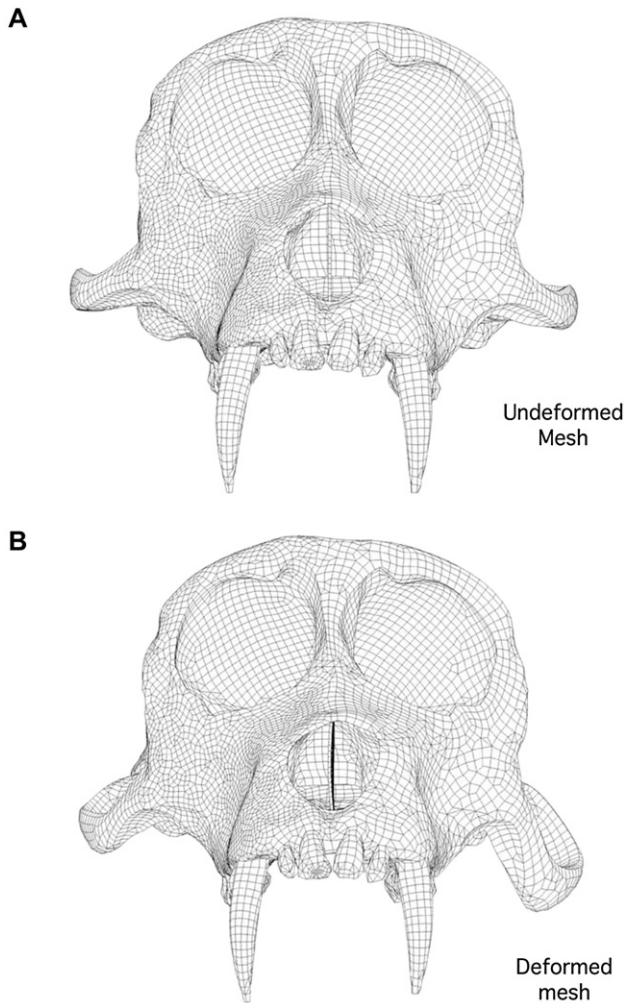


Fig. 5. Deformation: (A) frontal view of mesh prior to the application of loads; (B) frontal view of model after the application of loads, showing magnified deformation. Note that the zygomatic arches are displaced inferiorly, the working-side orbit is mediolaterally elongated and inferosuperiorly compressed, the balancing-side orbit is slightly inferosuperiorly elongated, and the rostrum is deformed such that the balancing-side tooth row is displaced inferiorly.

other facial regions require further explanation. Presumably, these increases are due to the fact that the palate in the THICK model is structurally more rigid than that in the NORMAL model. In a simple beam during bending, if a part of the beam is thickened, the remaining thinner sections will experience increased strain, and have stress concentrations in the transitional regions between the thick and thin sections. The facial skeleton is much more complex than a beam, but similar effects can be seen. In the bone immediately adjacent to the thickened areas (regions 14 and 15), strain is increased in the THICK model.

It is interesting that, like the palatal sites, some sites on the rostrum (regions 11, 12, and 13) have reduced strain, suggesting that the greater rigidity of the palate contributes to increased rigidity of much of the rostrum. On the other hand, the greater strains in the zygomatic and circumorbital regions suggest that, although the stress patterns in these

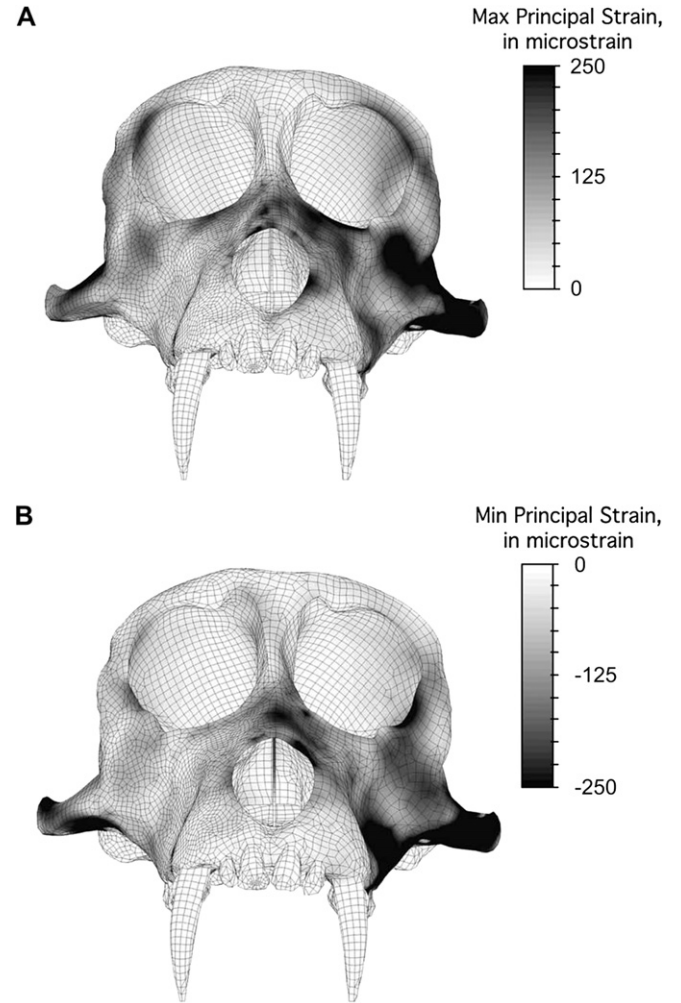


Fig. 6. Strain concentrations, frontal view: (A) maximum principal strain; (B) minimum principal strain.

regions are influenced by load transfer from the rostrum (maxilla), they represent at least a partially distinct structural unit. This interpretation is consistent with biomechanical models that predict that the mammalian secondary palate acts to stiffen and strengthen the rostrum so as to withstand torsional loads associated with mastication (Thomason and Russell, 1986).

Evaluation of the functional hypothesis

The functional hypothesis predicts that strains in the palate will be substantially decreased in the THICK model. This prediction was observed in the palatal regions where the bone was thickened (regions 16–18), and thus, in a strict sense, the hypothesis is corroborated. Nonetheless, interpreting a thick palate as an adaptation for withstanding masticatory stress is not straightforward because a thickened palate has the effect of increasing stress in other parts of the face. If the palate ordinarily experiences higher stresses than do other facial regions, then one might interpret palatal thickness as an adaptation to redistribute stress from areas of high stress to areas of lower

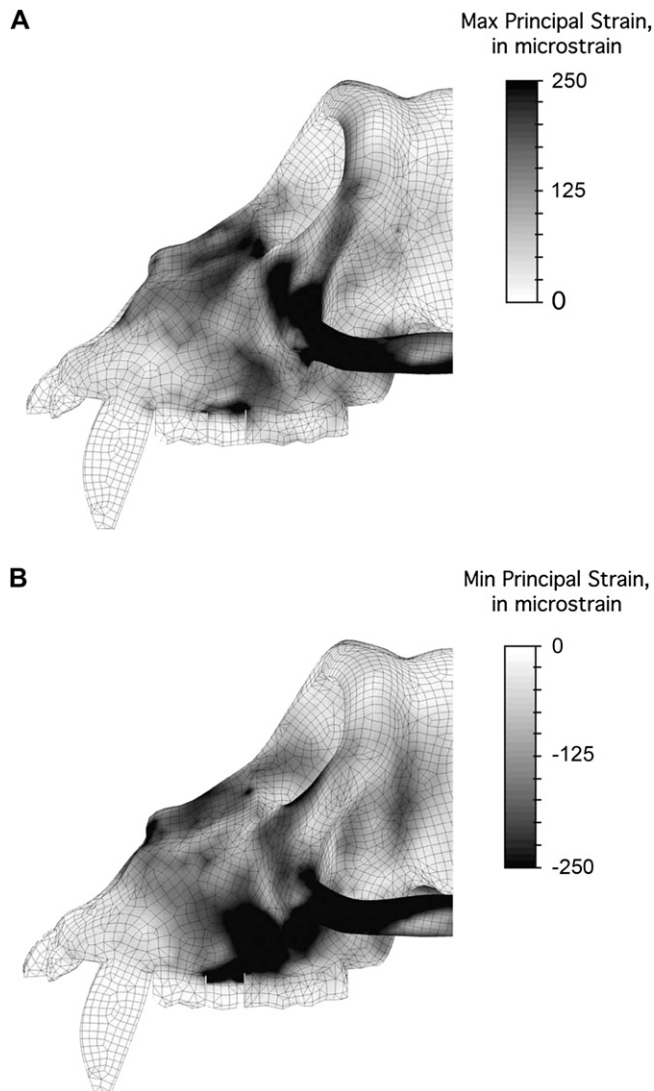


Fig. 7. Strain concentrations, lateral view, close-up view of face: (A) maximum principal strain; (B) minimum principal strain.

stress. Yet, in the NORMAL model, the palate does not exhibit strains that are markedly higher than in other parts of the face. Thus, it is not possible to interpret a thick palate in isolation as an adaptation for resisting masticatory stress.

It is possible, however, to view palatal thickness as a chewing adaptation if this morphology evolved in concert with other features that act to reduce stress across the face as a whole. For example, consider a primate whose dietary regime required the habitual production of high bite forces. These bite forces, and the associated high muscle forces, would elevate stress in many facial regions. As a result, stress-minimizing modifications in morphology might be a response in those regions. Thickening the palate reduces stress in this area, but has the effect of increasing stress in other areas. Those regions would therefore require modifications that accommodate not only the stress imposed by the high bite force, but also that imposed by having a rigid palate. In this regard, it is worth noting that a thick palate does not appear in early hominids without also being associated with

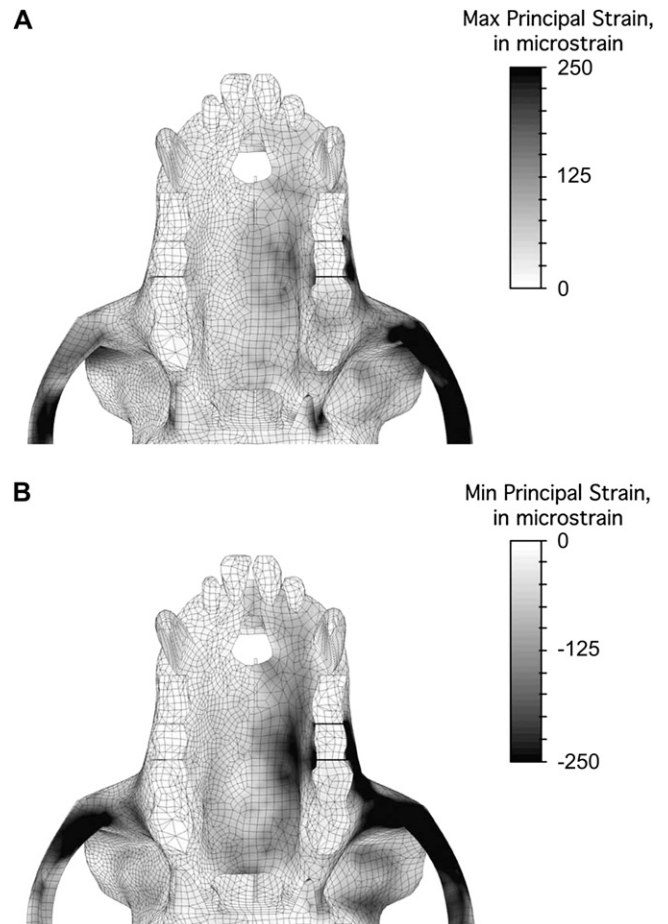


Fig. 8. Strain concentrations, palatal view, close-up view of face: (A) maximum principal strain; (B) minimum principal strain.

other derived facial features. A thick palate is only present in *Paranthropus*, and *Paranthropus* shares a suite of facial features not seen in other hominids. Moreover, *Paranthropus* had massive masticatory muscles and presumably was able to generate high bite forces. If future studies demonstrate that many facial features in *Paranthropus* act to reduce stress, then they can be viewed collectively as a global response to elevated bite forces in this genus.

Implications for early hominid phylogeny

The interpretation described above implies that a thick palate would not evolve independently as an adaptation to reduce chewing stress. Rather, it should evolve only in conjunction with other stress-reducing facial features. It follows that natural selection should favor the evolution of morphological integration (e.g., Olson and Miller, 1958; Cheverud, 1982, 1996; Chernoff and Magwene, 1999) among such features, even if those features are found in different structural units of the face. Thus, this study provides tacit support for the premise that some masticatory features might be expected to be morphologically integrated, and should be downweighted in a phylogenetic analysis (Skelton et al., 1986; Skelton and McHenry, 1992). Integration among masticatory features would weaken

Table 3
Strain data from locations on NORMAL model

Location ¹	Maximum principal strain ²	Intermediate principal strain ²	Minimum principal strain ²	Maximum shear strain ^{2,3}	Orientation of maximum principal strain (x, y, z) ⁴
1. Dorsal interorbital	47	-4	-17	64	(0.98, 0.08, 0.17)
2. W Dorsal orbital	44	-2	-40	84	(0.74, 0.31, 0.60)
3. B Dorsal orbital	38	-2	-34	72	(0.86, -0.29, -0.43)
4. W Infraorbital	290	-54	-179	469	(0.81, 0.39, -0.45)
5. B Infraorbital	140	-19	-86	226	(0.82, -0.22, 0.53)
6. W Midzygomatic	503	-17	-435	938	(0.32, 0.80, -0.51)
7. B Midzygomatic	85	50	-188	272	(0.67, 0.66, -0.35)
8. W Postorbital bar	129	-8	-107	237	(0.53, 0.83, 0.19)
9. Dorsal rostrum	138	-34	-173	311	(0.96, 0.11, -0.26)
10. W Lateral rostrum	196	-37	-100	296	(0.55, -0.01, -0.84)
11. B Lateral rostrum	28	-6	-16	44	(-0.61, -0.79, 0.09)
12. W Buccal alveolus	112	1	-120	232	(0.55, 0.13, -0.83)
13. B Buccal alveolus	20	5	-36	56	(0.71, -0.67, 0.24)
14. W Palatal margin	82	33	-162	243	(0.88, -0.47, -0.09)
15. B Palatal margin	24	0	-19	43	(0.21, 0.05, 0.96)
16. W Palatine process	105	44	-144	248	(0.78, -0.56, -0.29)
17. B Palatine process	21	8	-44	65	(0.58, 0.28, 0.77)
18. Midpalate	70	26	-79	150	(0.92, 0.38, 0.12)

¹ W = working-side; B = balancing-side.

² Measured in microstrain.

³ Defined as maximum principal strain minus minimum principal strain.

⁴ X-direction is positive to the left (working) side; y-direction is positive superiorly; z-direction is positive anteriorly.

support for hypotheses stating that such features are homologous in *Paranthropus* (e.g., Strait et al., 1997). However, this study does not actually demonstrate that the features in question are integrated. For example, certain masticatory characters could be used in different combinations to achieve the same functional goal (in this case, stress resistance). Such characters would not necessarily evolve in unison, and thus, might not be integrated. In order to fully evaluate the phylogenetic hypotheses that rely upon the integration of masticatory features, the functional relationships of more facial features need to be established, and formal studies of morphological integration (e.g., Cheverud, 1982, 1984; Zelditch, 1987, 1988; Fink and Zelditch, 1996; Ackermann and Cheverud, 2000) need to be performed.

The present study implies that palatal thickness may play a role in resisting chewing loads, and thus, for this feature, does not allow rejection of the hypothesis that the *Paranthropus* face is prone to homoplasy because its morphology is functionally related to mastication (Walker et al., 1986). However, the key premise of this hypothesis is that function induces homoplasy, and this premise should be tested using a combination of functional and phylogenetic methods. It is noteworthy, however, that Collard and Wood (2001), using primarily phylogenetic methods, found results inconsistent with the premise.

The results found here do not contradict the hypothesis that the palate may be developmentally integrated with other facial features (McCullum, 1999), but they do contradict the notion that changes in palatal thickness lack functional consequences related to mastication. This suggests that there is unlikely to be a straightforward dichotomy between developmentally and functionally integrated features in the hominoid face (contra

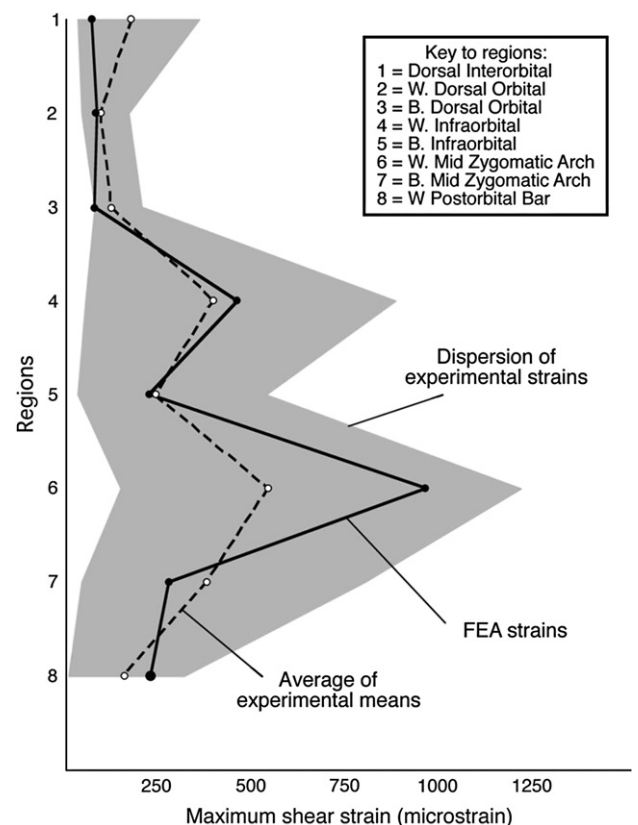


Fig. 9. Validation (shear-strain magnitude). Strains obtained from FEA shown as solid line. Average of the mean strains obtained in in vivo experiments (Hylander et al., 1991; Hylander and Johnson, 1997; Ross et al., 2002; Ross et al., unpublished data) shown as dashed line. Shaded area represents the range encompassed by the mean plus or minus two standard deviations of each experiment.

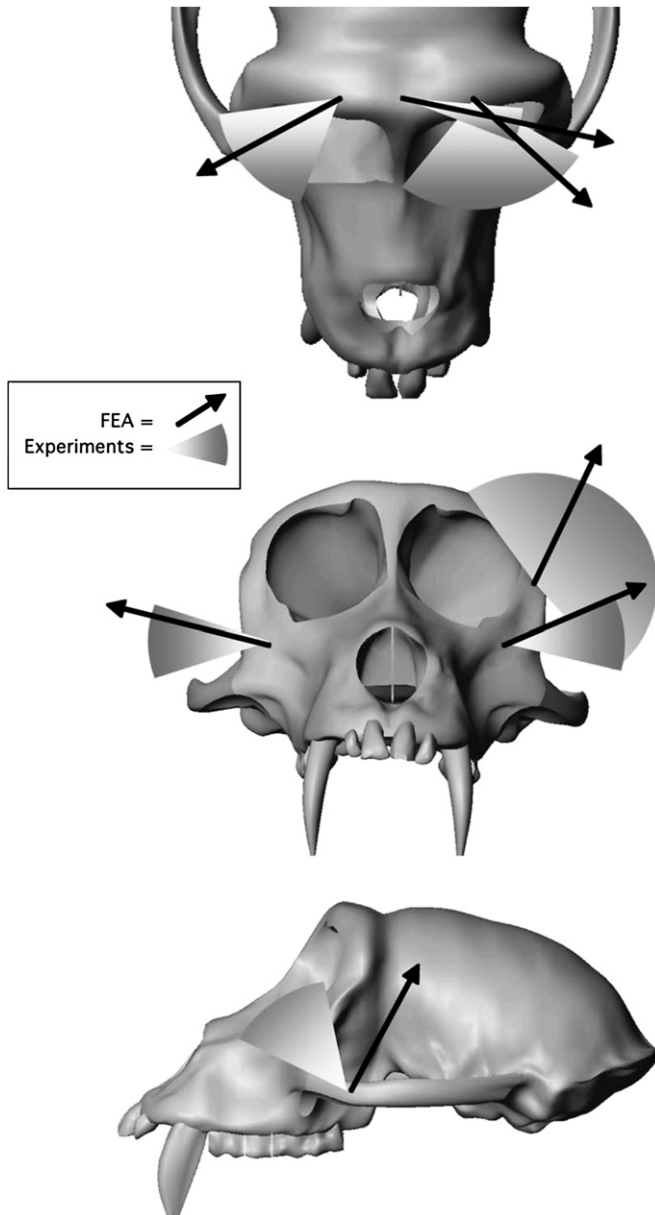


Fig. 10. Validation (orientation of maximum principal strain). Strains obtained from FEA shown as arrows. Range of experimental strains calculated using the mean plus or minus two standard deviations of each experiment (Hylander et al., 1991; Hylander and Johnson, 1997; Ross et al., 2002; Ross et al., unpublished data).

McCollum, 1999). Rather, integration may be the result of a complex interplay between both development and function. For example, the developmental integration proposed by McCollum (1999) may be the mechanism through which functional integration is achieved. Finally, the present study implies that the assumption of character independence implicit in cladistic analyses should not be accepted uncritically. Thus, phylogenetic reconstructions obtained under the premise that characters are independent until proven otherwise (e.g., Strait et al., 1997; Strait and Grine, 1999, 2001, 2004) should be viewed as hypotheses to be tested by future studies of function, development, and integration.

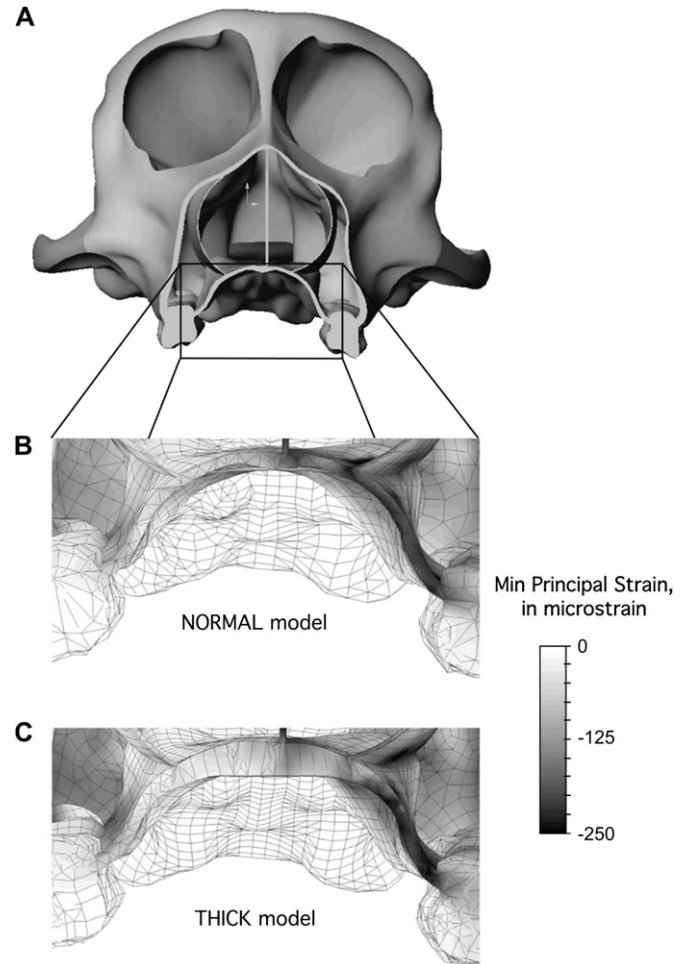


Fig. 11. Cross section through palate at M^1 : (A) solid NORMAL model; (B) mesh of NORMAL model, showing minimum principal strain; (C) mesh of THICK model, showing minimum principal strain. Relative to NORMAL model, strains in THICK model are reduced in the center of the palate where bone has been thickened, but elevated in the margins of the palate where bone thickness has not changed.

Conclusion

The present study does not establish definitively whether palatal thickness and other facial features evolved homoplastically in early hominids. Rather, it provides an initial step towards resolving this issue by testing whether a thick palate plays a role in stress-resistance during mastication. Future studies must establish the functional relationships of other facial characters, and hypotheses purporting to explain the developmental bases of specific facial features need to be tested. Following this, formal studies of morphological integration must be undertaken, and the role of function in inducing homoplasy must be evaluated. Once these research goals are achieved, systematists will be able to select characters secure in the knowledge that their choices will not unduly bias the results of a cladistic analysis. Ultimately, the question of whether hominid masticatory features are homoplastic will be resolved by informed phylogenetic analysis.

Table 4
Strain data from locations on THICK model

Location ¹	Maximum principal strain ²	Intermediate principal strain ²	Minimum principal strain ²	Maximum shear strain ^{2,3}	Orientation of maximum principal strain (x, y, z) ⁴
1. Dorsal interorbital	64	-5	-25	89	(0.98, 0.08, 0.20)
2. W Dorsal orbital	40	11	-69	108	(0.63, 0.57, 0.52)
3. B Dorsal orbital	43	6	-50	93	(0.84, -0.33, -0.44)
4. W Infraorbital	389	-78	-190	579	(0.80, 0.39, -0.45)
5. B Infraorbital	164	-34	-94	258	(0.83, -0.19, 0.53)
6. W Midzygomatic	535	48	-535	1069	(0.41, 0.80, -0.44)
7. B Midzygomatic	93	41	-191	284	(0.66, -0.72, 0.20)
8. W Postorbital bar	168	-14	-128	296	(0.47, 0.86, 0.17)
9. Dorsal rostrum	126	-100	-161	287	(0.40, -0.79, 0.47)
10. W Lateral rostrum	175	-29	-81	256	(0.42, -0.11, -0.90)
11. B Lateral rostrum	20	3	-21	41	(0.71, -0.71, 0.04)
12. W Buccal alveolus	140	-3	-111	251	(0.77, -0.12, -0.63)
13. B Buccal alveolus	28	1	-33	62	(0.85, -0.51, 0.15)
14. W Palatal margin	105	23	-206	310	(0.82, -0.57, 0.01)
15. B Palatal margin	25	8	-30	55	(0.39, 0.05, 0.92)
16. W Palatine process	44	16	-96	141	(0.58, -0.72, 0.39)
17. B Palatine process	26	3	-14	39	(0.89, 0.06, 0.46)
18. Midpalate	61	8	-41	101	(0.93, 0.06, 0.37)

¹ W = working-side; B = balancing-side.

² Measured in microstrain.

³ Defined as maximum principal strain minus minimum principal strain.

⁴ X-direction is positive to the left (working) side; y-direction is positive superiorly; z-direction is positive anteriorly.

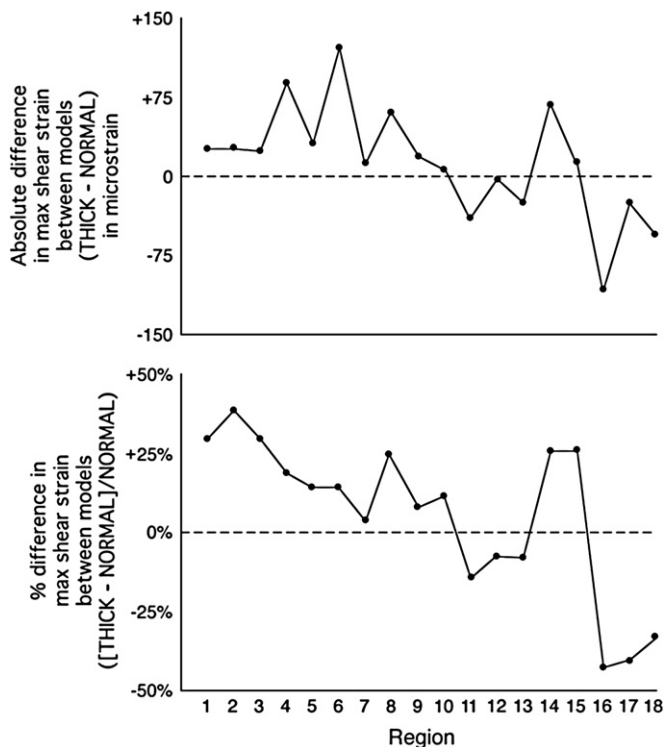


Fig. 12. THICK vs. NORMAL models (maximum shear strain): (A) absolute difference between models—magnitude of shear strain in THICK model minus magnitude in NORMAL model; (B) percentage difference between models—difference calculated in A as a percentage of magnitude in NORMAL model. Regions as in Fig. 5. In both A and B, positive values indicate that strains are higher in the THICK models, while negative values indicate that strains are higher in the NORMAL model.

Acknowledgements

The authors thank the organizers of the conference for their generous invitation to attend, and for their profound patience while awaiting the initial draft of this paper. Thanks also to the participants of the conference for many hours of insightful and enjoyable discussion. R. Thorington kindly allowed us access to specimens in his care at the National Museum of Natural History (NMNH) and B. Froelich allowed us to use the NMNH's CT-scanning equipment. This paper was improved considerably by comments from Y. Rak, D. Daegling, and an anonymous reviewer. This research was supported in part by The Henry Luce Foundation. In vivo macaque data were collected using funding from an NSF Physical Anthropology Grant to C. Ross and X. Chen (SBR 9706676). Finite-element analysis was supported by an NSF Physical Anthropology grant to D. Strait, P. Dechow, B. Richmond, C. Ross, and M. Spencer (BCS 0240865).

References

- Ackermann, R.R., Cheverud, J.M., 2000. Phenotypic covariance structure in tamarins (genus *Saguinas*): a comparison of variation patterns using matrix correlation and common principal components analysis. *Am. J. Phys. Anthropol.* 111, 489–501.
- Anton, S.C., 1993. Internal masticatory muscle architecture in the Japanese macaque and its influence on bony morphology. *Am. J. Phys. Anthropol.* 16 (Suppl.), 50.
- Begun, D.R., 2007. How to identify (as opposed to define) a homoplasy: Examples from fossil and living great apes. *J. Hum. Evol.* 52, 559–572.
- Borrazzo, E.C., Hylander, W.L., Rubin, C.T., 1994. Validation of a finite element model of the functionally loaded zygomatic arch by in vivo strain gage data. *Proc. Am. Soc. Biomech.* 18, 51–52.

- Chamberlain, A.T., Wood, B.A., 1987. Early hominid phylogeny. *J. Hum. Evol.* 16, 119–133.
- Chen, X., Chen, H., 1998. The influence of alveolar structures on the torsional strain field in a gorilla corporeal cross-section. *J. Hum. Evol.* 35, 611–633.
- Chernoff, B., Magwene, P.M., 1999. Morphological integration: forty years later. In: Olson, E.C., Miller, R.L. (Eds.), *Morphological Integration*. University of Chicago Press, Chicago, pp. 319–348.
- Cheverud, J.M., 1982. Phenotypic, genetic, and environmental morphological integration in the cranium. *Evolution* 36, 499–516.
- Cheverud, J.M., 1984. Quantitative genetics and developmental constraints on evolution by selection. *J. Theoret. Biol.* 110, 155–172.
- Cheverud, J.M., 1996. Developmental integration and the evolution of pleiotropy. *Am. Zool.* 36, 44–50.
- Cheverud, J., Lewis, J.L., Bachrach, W., Lew, W.D., 1983. The measurement of form and variation in form: An application of three-dimensional quantitative morphology by finite-element methods. *Am. J. Phys. Anthropol.* 62, 151–165.
- Collard, M., Wood, B.A., 2001. Homoplasy and the early hominid masticatory system: inferences from analyses of extant hominoids and papionins. *J. Hum. Evol.* 41, 167–194.
- Collard, M., Wood, B.A., 2007. Hominin homology: an assessment of the impact of phenotypic plasticity on phylogenetic analyses of humans and their fossil relatives. *J. Hum. Evol.* 52, 573–584.
- Cook, R.D., Malkus, D.S., Plesha, M.E., 1989. *Concepts and Applications of Finite Element Analysis*. John Wiley and Sons, New York.
- Cowin, S.C., 1989. Mechanics of materials. In: Cowin, S.C. (Ed.), *Bone Mechanics*. CRC Press, Inc., Boca Raton, pp. 15–42.
- Cracraft, J., 1981. The use of functional and adaptive criteria in phylogenetic systematics. *Am. Zool.* 21, 21–36.
- Currey, J., 1984. *The Mechanical Adaptations of Bones*. Princeton University Press, Princeton.
- Endo, B., 1966. Experimental studies on the mechanical significance of the form of the human facial skeleton. *J. Faculty Sci. Univ. Tokyo Section V III*, 1–106.
- Fink, W.L., Zelditch, M.L., 1996. Historical patterns of developmental integration in piranhas. *Am. Zool.* 36, 61–69.
- Greaves, W.S., 1985. The mammalian post-orbital bar as a torsion-resisting helical strut. *J. Zool. (Lond.)* 207, 125–136.
- Grine, F.E., 1981. Trophic differences between gracile and robust *Australopithecus*: a scanning electron microscope analysis of occlusal events. *S. Afr. J. Sci.* 77, 203–230.
- Gross, T.S., McLeod, K.J., Rubin, C.T., 1992. Characterizing bone strain distributions in vivo using three triple rosette strain gages. *J. Biomech.* 25, 1081–1087.
- Huiskes, R., Chao, E.Y.S., 1983. A survey of finite element analysis in orthopedic biomechanics: the first decade. *J. Biomech.* 16, 385–409.
- Hylander, W.L., 1984. Stress and strain in the mandibular symphysis of primates: a test of competing hypotheses. *Am. J. Phys. Anthropol.* 64, 1–46.
- Hylander, W.L., 1986. In vivo bone strain as an indicator of masticatory bite force in *Macaca fascicularis*. *Arch. Oral Biol.* 31, 149–157.
- Hylander, W.L., Johnson, K.R., 1989. The relationship between masseter force and masseter electromyogram during mastication in the monkey *Macaca fascicularis*. *Arch. Oral Biol.* 34, 713–722.
- Hylander, W.L., Johnson, K.R., 1997. In vivo bone strain patterns in the zygomatic arch of macaques and the significance of these patterns for functional interpretations of craniodental form. *Am. J. Phys. Anthropol.* 102, 203–232.
- Hylander, W.L., Picq, P.G., Johnson, K.R., 1991. Masticatory-stress hypotheses and the supraorbital region of primates. *Am. J. Phys. Anthropol.* 86, 1–36.
- Jolly, C.J., 1970. The seed eaters: a new model for hominid differentiation based on a baboon analogy. *Man* 5, 5–26.
- Kitching, I.J., Forey, P.L., Humphries, C.J., Williams, D.M., 1998. *Cladistics*. Oxford University Press, Oxford.
- Koricho, T.W.P., Romilly, D.P., Hannam, A.G., 1992. Three-dimensional finite element stress analysis of the dentate human mandible. *Am. J. Phys. Anthropol.* 88, 69–96.
- Lauder, G.V., 1994. Homology, form, and function. In: Hall, B.K. (Ed.), *Homology: The Hierarchical Basis of Comparative Biology*. Academic Press, San Diego, pp. 152–197.
- McCollum, M.A., 1999. The robust australopithecine face: a morphogenetic perspective. *Science* 284, 301–305.
- McCollum, M.A., Grine, F.E., Ward, S.C., Kimbel, W.H., 1993. Subnasal morphological variation in extant hominoids and fossil hominids. *J. Hum. Evol.* 24, 87–111.
- Murphy, R.A., 1998. Skeletal muscle. In: Berne, R.M., Levy, M.N. (Eds.), *Physiology*. Mosby, St. Louis, p. 294.
- Olson, E., Miller, R., 1958. *Morphological Integration*. University of Chicago Press, Chicago.
- Peterson, J., Dechow, P.C., 2003. Material properties of the human cranial vault and zygoma. *Anat. Rec.* 274A, 785–797.
- Preuschoft, H., Demes, B., Meyer, H., Bar, H.F., 1986. The biomechanical principles realized in the upper jaw of long-snouted primates. In: Else, J.G., Lee, P.C. (Eds.), *Primate Evolution*. Cambridge University Press, Cambridge, pp. 249–264.
- Rak, Y., 1983. *The Australopithecine Face*. Academic Press, New York.
- Rayfield, E.J., Norman, D.B., Horner, C.C., Horner, J.R., Smith, P.M., Thomason, J.J., Upchurch, P., 2001. Cranial design and function in a large theropod dinosaur. *Nature* 409, 1033–1037.
- Richmond, B.G., 1998. Ontogeny and biomechanics of phalangeal form in primates. Ph.D. Dissertation, Stony Brook University.
- Richmond, B.G., Qin, Y.-X., 1996. Finite element methods in paleoanthropology: the case of phalangeal curvature. *Am. J. Phys. Anthropol.* 22 (Suppl.), 197.
- Richmond, B.G., Wright, B.W., Grosse, I., Dechow, P.C., Ross, C.F., Spencer, M.A., Strait, D.S., 2005. Finite element analysis in functional morphology. *Anat. Rec.* 283A, 259–274.
- Richstmsmeier, J.T., Cheverud, J.M., Lele, S., 1992. Advances in anthropological morphometrics. *Annu. Rev. Anthropol.* 21, 283–305.
- Robinson, J.T., 1954. Prehominid dentition and hominid evolution. *Evolution* 8, 324–334.
- Robinson, J.T., 1963. Adaptive radiation in the australopithecines and the origin of man. In: Howell, F.C., Boulière, F. (Eds.), *African Ecology and Human Evolution*. Aldine, Chicago, pp. 385–416.
- Ross, C.F., 2001. In vivo function of the craniofacial haft: the interorbital “pillar”. *Am. J. Phys. Anthropol.* 116, 108–139.
- Ross, C.F., Chen, X., 1997. A finite element model of the owl monkey circumorbital region: comparison with in vivo and in vitro bone strain data. *Am. J. Phys. Anthropol.* 24 (Suppl.), 200.
- Ross, C.F., Hylander, W.L., 1996. In vivo and in vitro bone strain in the owl monkey circumorbital region and the function of the postorbital septum. *Am. J. Phys. Anthropol.* 101, 183–215.
- Ross, C.F., Patel, B.A., Slice, D.E., Strait, D.S., Dechow, P.C., Richmond, B.G., Spencer, M.A., 2005. Modeling masticatory muscle force in finite element analysis: sensitivity analysis using principal coordinates analysis. *Anat. Rec.* 283A, 288–299.
- Ross, C.F., Strait, D.S., Richmond, B.G., Spencer, M.A., 2002. In vivo bone strain and finite-element modeling of the anterior root of the zygoma of *Macaca*. *Am. J. Phys. Anthropol.* 34 (Suppl.), 133.
- Ryan, T.M., Kappelman, J., 1997. A structural analysis of tibial shape using the finite element method. *Am. J. Phys. Anthropol.* 24 (Suppl.), 202.
- Skelton, R.R., McHenry, H.M., 1992. Evolutionary relationships among early hominids. *J. Hum. Evol.* 23, 309–349.
- Skelton, R.R., McHenry, H.M., 1998. Trait list bias and a reappraisal of early hominid phylogeny. *J. Hum. Evol.* 34, 109–113.
- Skelton, R.R., McHenry, H.M., Drawhorn, G.M., 1986. Phylogenetic analysis of early hominids. *Curr. Anthropol.* 27, 329–340.
- Spears, I.R., Crompton, R.H., 1994. Finite elements stress analysis as a possible tool for reconstruction of hominid dietary mechanics. *Z. Morphol. Anthropol.* 80, 239–254.
- Spears, I.R., Crompton, R.H., 1996. The mechanical significance of the occlusal geometry of great ape molars in food breakdown. *J. Hum. Evol.* 31, 517–535.
- Strait, D.S., Grine, F.E., 1998. Trait list bias? A reply to Skelton and McHenry. *J. Hum. Evol.* 34, 115–118.

- Strait, D.S., Grine, F.E., 1999. Cladistics and early hominid phylogeny. *Science* 285, 1210.
- Strait, D.S., Grine, F.E., 2001. The systematics of *Australopithecus garhi*. *Ludus Vitalis* 9, 17–82.
- Strait, D.S., Grine, F.E., 2004. Inferring hominoid and early hominid phylogeny using craniodental data: the role of fossil taxa. *J. Hum. Evol.* 47, 399–452.
- Strait, D.S., Grine, F.E., Moniz, M.A., 1997. A reappraisal of early hominid phylogeny. *J. Hum. Evol.* 32, 17–82.
- Strait, D.S., Wang, Q., Dechow, P.C., Ross, C.F., Richmond, B.G., Spencer, M.A., Patel, B.A., 2005. Modeling elastic properties in finite-element analysis: how much precision is needed to produce an accurate model? *Anat. Rec.* 283A, 275–287.
- Thomason, J.J., Russell, A.P., 1986. Mechanical factors in the evolution of the mammalian secondary palate: a theoretical analysis. *J. Morphol.* 189, 199–213.
- Wainwright, S.A., Biggs, W.D., Currey, J.D., Gosline, J.M., 1982. *Mechanical Design in Organisms*. Princeton University Press, Princeton.
- Walker, A., 1981. Dietary hypotheses and human evolution. *Philos. Trans. R. Soc. (Lond.) B* 292, 57–64.
- Walker, A.C., Leakey, R.E.F., Harris, J.M., Brown, F.H., 1986. 2.5-Myr *Australopithecus boisei* from west of Lake Turkana, Kenya. *Nature* 322, 517–522.
- Wang, Q., Dechow, P.C., 2006. Elastic properties of external cortical bone in the craniofacial skeleton of the rhesus monkey. *Am. J. Phys. Anthropol.* 131, 402–415.
- White, T.D., Johanson, D.C., Kimbel, W.H., 1981. *Australopithecus africanus*: Its phyletic position reconsidered. *S. Afr. J. Sci.* 77, 445–470.
- Wood, B.A., 1988. Are “robust” australopithecines a monophyletic group? In: Grine, F.E. (Ed.), *Evolutionary History of the “Robust” Australopithecines*. Aldine de Gruyter, New York, pp. 269–284.
- Wood, B.A., 1991. *Koobi Fora Research Project, Vol. 4: Hominid Cranial Remains*. Clarendon, Oxford.
- Wood, B.A., 1992. Early hominid species and speciation. *J. Hum. Evol.* 22, 351–365.
- Zelditch, M.L., 1987. Evaluating models of developmental integration in the laboratory rat using confirmatory factor analysis. *Syst. Zool.* 36, 368–380.
- Zelditch, M.L., 1988. Ontogenetic variation in patterns of phenotypic integration in the laboratory rat. *Evolution* 42, 28–41.